

# The Cubic Curves Hysteresis Model of Steel Bridge Piers for Seismic Response Simulation



**Dang Ji**

Department of Civil and Environment Engineering Aichi Institute of Technology, Dangji1980@yahoo.ac.jp

**Tetsuhiko Aoki**

Department of Civil and Environment Engineering Aichi Institute of Technology, Aoki@aitech.ac.jp

---

## Abstract

In this paper, a cubic type curve approximate hysteretic model for steel bridge pier is proposed. Simple equation curves are used to express restoring force-displacement relation of steel piers. The hysteretic rules introduced in this model are established based on the hysteretic characteristics not only observed from quasi-static tests in past, but also based on conducted hybrid tests in this study. A series of quasi-static tests and hybrid tests are conducted using 3 types of specimens and 6 accelerograms of strong ground motions. By comparing the results of tests and the simulation, it has been testified that this cubic curve type model can simulate the inelastic hysteresis behavior and earthquake response of steel piers in high precise, even in large displacement range where the piers experience local buckling near to collapse.

---

**Keywords:** Steel bridge pier, hysteretic model, hybrid test, cubic curve approximation

## 1. Introduction

The Kobe earthquake Japan, in 1995, had experienced extremely economical lost due to delay of the urgent support and loss of function of transportation, because of the collapse of high-way bridges. To maintain the function of high-way road, the improvement of the seismic guard of viaduct bridge piers becomes one of very important issues.

Usami et al (1991, 1992, 1993), Suzuki et al. (1995), Aoki et al. (2007) have been conducted a lot of quasi-static tests to clarify the seismic performance of steel piers so far. These tests were performed under increasing cyclic displacements, so that the basic load-displacement behavior can be obtained easily. But it is very difficult to clarify the inelastic responses of steel piers subjected actual earthquake ground motions by this kind of tests.

The hybrid test, on the other hand, is able to investigate the complicated inelastic responses of steel piers, which have been applied by Iemura (1985), Saizuka (1995), Usami (1995). The hybrid test solves the vibration function by computer and measures restoring force of the test pier caused by the predicted displacements to the test model. As results of hybrid test on steel piers, it is very

difficult to predict the inelastic response of steel pier by simplified method, like energy conservation method or simulation by perfect elastic-plastic like bi-linear model. Suzuki M. et al. (1996) proposed a tri-linear type hysteretic model for steel pier, in which some hysteretic rules were proposed to introduce the hardening and deteriorate characters of steel piers. A few methods based on energy absorption were proposed, so far, to predict deterioration behavior of peak load point after local buckling.

Kindaich T. et al (1998) also proposed another tri-linear type hysteretic model based on the damage index. The damage index indicates the damage level that a steel pier suffered in earthquakes. This hysteretic model can introduce the deterioration of the stiffness and the peak load of steel pier as the synchronous increasing of damage index.

Both of these hysteretic models are established based on tri-linear approximation, which cause difference from the continuous hysteretic curve of steel pier in some regions and generate error in energy absorption accumulating to noticeable level.

On the other hand, Dang J. et al (2009) proposed a multi-curve model for steel pier columns. It was clarified by comparing the result of hysteretic model with

quasi-static tests that the polynomial curve approximation can high-similarly express the load-displacement relation of steel pier. But the details of this model are still need revises, and the accuracy of this model has not been testified by hybrid tests.

In this paper, by revising the multi-curve model and simplify its procedure, the hysteretic model that expresses the load-displacement relationship of steel pier by simple mathematic function curves is proposed.

To discuss the precision of the hysteresis model using cubic curves, a series of quasi-static tests and hybrid tests are conducted by large scale loading system in the Seismic Resistance Experiment Center (SREC) of Aichi Institute of Technology.

## 2. Cubic curve hysteretic model for steel bridges

The cubic curve hysteretic model for steel piers is constituted of raising curves and deterioration curves. As shown in Figure 1, a raising curve is a part of hysteretic curve before peak load, where the gradient (stiffness) is positive. A deterioration curve is a part of a hysteretic curve after the peak load, where the gradient (stiffness) is negative.

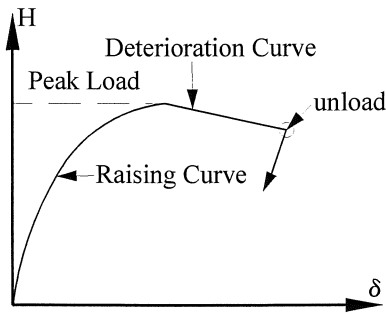


Figure 1. The constitution of a hysteretic loop

### 2.1. Raising curves

Many Japanese researchers (Usami T., 1991, 1992, 1993; Suzuki M. (1995); Iura M., 1997, ect.) have conducted monotonic and cyclic loading tests for steel pier columns. It was found from these tests that, even in different loading patterns, the normalized peak loads ( $H_{m0}/H_y$ ) and the corresponding displacements ( $\delta_{m0}/\delta_y$ ) of steel piers are considered to be almost constant. This characteristic is applied as the basic hysteretic rule of the cubic curve hysteretic model presented here.

We define the curves reaching peak load point ( $\delta_m, H_m$ ) as “basic curve”, and the curves applied to unload-reloading path as “sub curve”. A basic curve is expressed by a cubic equation of which terminal point is the peak load point, and a sub curve is used as a quadratic equation of which terminal point is the unloaded point.

#### 2.1.1 The basic curve

The curves numbered as 1, 2 and 4 are basic curves in

Fig.2, where the vertical axis illustrates the horizontal force  $H$  and the horizontal axis indicates the displacement  $\delta$ . The curve 1 is a hysteresis curve loading from the origin point  $O$  to the peak point  $M(+)(\delta_m, H_m)$ . In this figure, The basic curve 1 can be approximated by the following cubic type equation.

$$H = K_e \delta + \alpha_1 \delta^2 + \alpha_2 \delta^3 \quad (1)$$

where,  $K_e$  is the elastic stiffness. In Eq. (1), the parameter  $\alpha_1$  and  $\alpha_2$  can be obtained by following conditions.

I The basic curve passes through the peak load point.  
( $H_m = K_e \delta_m + \alpha_1 \delta_m^2 + \alpha_2 \delta_m^3$ )

II The gradient of this curve is zero at the peak load point.

$$(K_e + 2\alpha_1 \delta_m + 3\alpha_2 \delta_m^2 = 0)$$

Thus  $\alpha_1$  and  $\alpha_2$  can be determined by the following equations.

$$\alpha_1 = 3H_m/\delta_m^2 - 2K_e/\delta_m \quad (2)$$

$$\alpha_2 = K_e/\delta_m^2 - 2H_m/\delta_m^3 \quad (3)$$

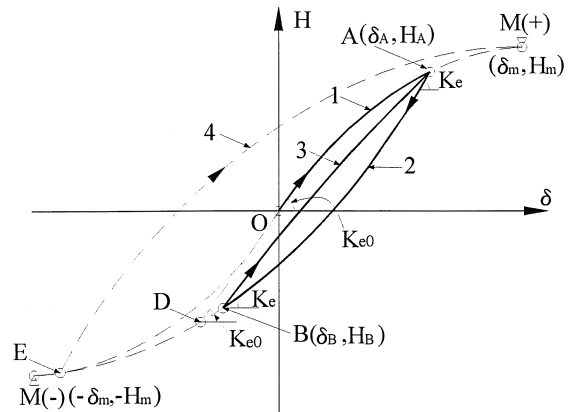


Figure 2. Raising curves

When unloading happened at point  $A(\delta_A, H_A)$  in the curve 1, as shown in Figure 2, the loading direction reversed to minus. From the point  $A$ , a new curve (the curve 2 in Figure 2) can be approximated by the same equation, but the values of  $H$ ,  $\delta$ ,  $H_m$  and  $\delta_m$  in Eq. (1)~(3) should be converted to the relative value of the start point of the curve (point  $A$ ). Derivation of these values ( $H_m, \delta_m$ ) will be demonstrated in the next chapter.

#### 2.1.2. The sub curve

Following a gradually increasing loading pattern, like a quasi-static test, the new hysteretic curve envelopes or traces the old ones, before peak load. But following a random loading path, like a hybrid test, some hysteretic curves appear inside old curves.

A sub curve is a hysteretic curve which connects two unloaded points and appears slower stiffness decreasing than a basic curve.

For example an unloading happens at point  $B$  on basic

curve 2 in Figure 2, a gradually increasing loading path is obtained by connecting unloaded points A and B by sub curve. The loading path after unloaded point A will go forward following the original basic curve 1 until peak load point M(+). This sub curve can also be expressed by the Eq. (1). Because it is usually difficult to find the gradient of the sub curve at the starting point A, for determining the equation of the curve using Eq. (1), the third term coefficient  $\alpha_2$  in the Eq. (1) is dropped and the coefficient  $\alpha_1$  is found as following.

$$\alpha_1 = (H_A - H_B)/(\delta_A - \delta_B)^2 - K_e/(\delta_A - \delta_B) \quad (4)$$

A limit unloading point D can be defined as a special point to separate the region defining the sub curve. Dragging a basic curve from point D, this basic curve will cover the old basic curve 1. Approximately, this limit point D can be determined as the intersection point of the current basic curve (curve 2) and the tangent line at the starting point of the initial basic curve (point O in curve 1).

Provide the unloading basic curves will be used after limit point D, then the curve 4 in Figure 2, for example, will be determined as a basic curve. On the other hand, when unloading is before point D, the loading curve is defined as sub curve, like curve 3 in Figure 2.

It means that, from an unloading point B, which is before limit point D, as shown in the figure, the loading follows the sub curve 3 until point A. After point A, loading path follows the rest part of the previous basic curve 1 (the part from point A to point M(+)).

If unloading happens before point A, the loading is following the sub curve at that time, so that another sub curve will be used to lead the loading to go back to point B, and so on.

## 2.2. Deterioration Curve

There are three considerations to determine the deterioration curve. To evaluate the deterioration behavior of steel pier, the effect of P- $\delta$  should firstly be considered, because the descending of horizontal force is not only caused by deterioration of capacity of the pier due to horizontal external force but also caused by P- $\delta$  effect due to the vertical force.

When the deformation of a pier becomes relatively large, the P- $\delta$  moment at base of piers will become more and more significant. Therefore, instead of using horizontal force directly, the "equivalent horizontal force", as mentioned hereafter, is introduced to evaluate the deterioration of capability of steel pier from results of quasi-static tests.

Secondly, the accumulation value of deterioration displacement is applied to evaluate the damage accumulation of steel pier column.

Finally, in the following section, the relationship of the accumulated deterioration displacement and equivalent horizontal force will be discussed, and an approximate equation to express this relationship is proposed to calculate the hysteretic curves in the deterioration region

(deterioration curves).

### 2.2.1. The equivalent horizontal force

Consider a pier, with effective height is  $h$ , subjected to a horizontal force  $H$  and a constant axis vertical force  $P$ , and caused horizontal displacement  $\delta$ , as illustrated in Figure 3. The moment at the base of the pier ( $M_B$ ) can be expressed by the following equation.

$$M_B = Hh + P\delta \quad (5)$$

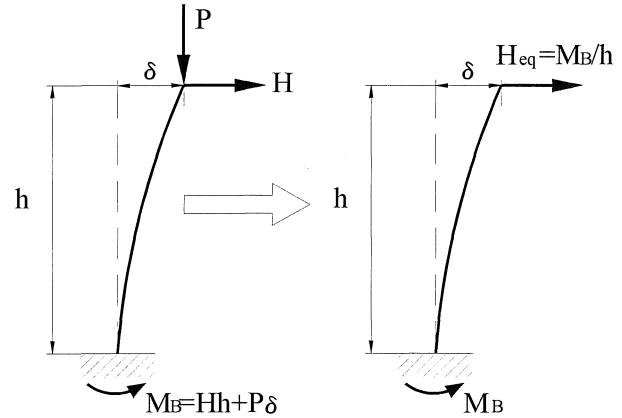


Figure 3. Definition of equivalent horizontal force  $H_{eq}$

If the horizontal force  $H$  descends with the increasing of horizontal displacement  $\delta$  in deterioration region, it could be deduced from Eq.(5) that this descending is not only caused by the descending of base resistance moment, but also caused by the increasing of P- $\delta$  moment.

Considering this, we define the equivalent horizontal force  $H_{eq}$  by the following equation to evaluate the descending of pier column's capacity.

$$H_{eq} = M_B = H + P\delta/h \quad (6)$$

### 2.2.2. The accumulated deterioration displacement

Figure 4 shows a half cyclic hysteretic curve containing a deterioration part. The deterioration starts from the peak load point M( $\delta_m, H_m$ ) and ends at the unloading point U( $\delta_u, H_u$ ). The displacement length experienced in this deterioration part can be expressed as  $\delta_p = \delta_u - \delta_m$ . Let the deterioration displacement experienced in the  $i^{\text{th}}$  cycle is denoted as  $\delta_p^{(i)}$ . After  $n$  cycles, once the displacement go further than the displacement at the peak load of the present cyclic ( $\delta_m$ ), the accumulated deterioration displacement  $\sum \delta_d$  is updated by the following equation using the present displacement  $\delta$ .

$$\sum \delta_d = \sum |\delta_p^{(i)}| + |\delta - \delta_m| \quad (7)$$

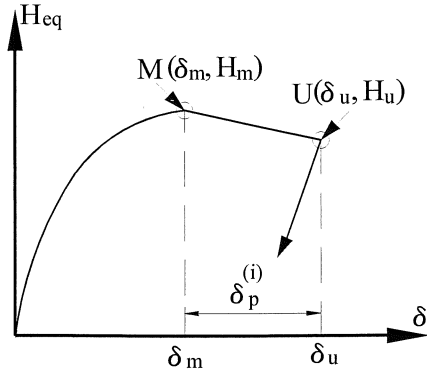


Figure 4. Deterioration displacement

### 2.2.3. Deterioration curve

A quadratic equation is proposed as following to describe the relationship between the equivalent horizontal force  $H_{eq}$  and the accumulated deterioration displacement  $\sum \delta_d$ ,

$$H_{eq}/H_y = H_{eq,m}/H_y + \beta_1 \sum \delta_d / \delta_y + \beta_2 (\sum \delta_d / \delta_y)^2 \quad (8)$$
 where  $H_{eq,m}$  is the initial maximum value of equivalent horizontal force that can be obtained by following equation,

$$H_{eq,m} = H_{m0} + P \delta_{m0} / h \quad (9)$$

where  $\delta_{m0}$  and  $H_{m0}$  is the displacement and the horizontal force of the initial peak load point that can be obtained by a cyclic loading test (quasi-static test) or FEM cyclic loading analysis. The parameter  $\beta_1$  and  $\beta_2$  can be determined by the least-squares method from the quasi-static loading test data.

The deterioration curve, which is the H- $\delta$  relationship starting from peak load point until unloading, can be obtained by the following procedure.

- I Calculate the accumulated deterioration displacement ( $\sum \delta_d$ ) by Eq.(7).
- II Substitute  $\sum \delta_d$  into Eq.(8) to estimate the equivalent horizontal force  $H_{eq}$ .
- III Calculate the horizontal force  $H$  by Eq.(6).

### 2.3. After Deterioration

The deterioration of horizontal force is normally caused by local buckling at the near bottom of the piers. Once the pier experienced deterioration, even in only one loading direction, deterioration of the stiffness and decline of the peak load can be observed in both loading directions. After deterioration, the raising curves still follow the basic hysteretic rules as mentioned before. However, the updates of peak load points and the stiffness are necessary.

#### 2.3.1. Deterioration of elastic stiffness

It can be approximately assumed that the elastic stiffness  $K_e$  deteriorates linearly with the increasing of the accumulated deterioration displacement  $\sum \delta_d$ . This

relationship can be approximated by the following linear equation.

$$K_e / K_{e0} = 1 + \gamma \sum \delta_d / \delta_y \quad (10)$$

where  $K_{e0}$  is the initial elastic stiffness, and the slope parameter  $\gamma$  can be determined from the quasi-static test by least-square method.

#### 2.3.2. The Update of peak load point

An example of hysteretic curve for the pier experienced deterioration in plus direction is shown in Figure 5. From point A in this figure, a hysteretic curve  $AM'_2$  can be obtained as a basic curve, where the point  $M'_2$  is the peak load point of the minus direction after deterioration. In this way, when the pier had experienced deterioration in plus side, the peak load point in minus side moves from original peak point  $M_2$  to a new peak point  $M'_2$ , as illustrated in this figure. The equivalent horizontal force  $H'_{eq,M2}$  at point  $M'_2$  can be approximately assumed as same as the value  $H_{eq,A}$  at point A. That is,

$$H'_{eq,M2} = H_{eq,A} \quad (11)$$

It has been observed from many test results that peak load of equivalent horizontal force  $H_{eq}$  in both plus and minus direction will be considered descending equally.

It is also assumed that the displacement of peak point will change from  $\delta_{m,2}$  to  $\delta'_{m,2}$ , as illustrated in Figure 7. The distance  $\delta_p^*$  between displacement of the original peak load point  $M_2$  and that of new peak load point  $M'_2$  can be expressed as following.

$$\delta_p^* = \delta_{m,2} - \delta'_{m,2} \quad (12)$$

The value of  $\delta_p^*$  can be predicted by examine the relationship with the experienced deterioration displacement  $\delta_p$  in the last hysteretic loop. The relationship of  $\delta_p^*$  with  $\delta_p$  is assumed as following,

$$\delta_p^* = \mu \delta_p \quad (13)$$

where the parameter  $\mu$  can be obtained by least-square method from test data.

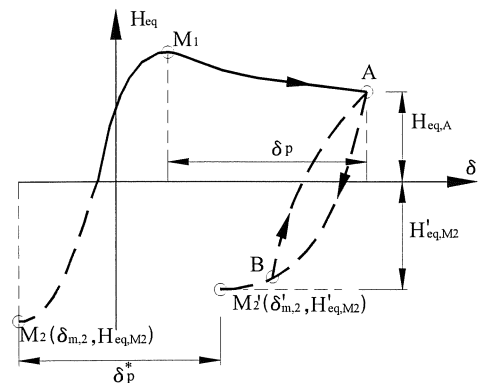


Figure 5. Hysteretic rules after deterioration

The basic curve could be obtained for the region from the unloading point A to the peak point  $M'_2$ . It means

that the new peak load point of plus direction, which was the point  $M_1$ , will be updated to the unloading point A.

#### 2.4. Parameters for hysteresis model

As stated above, to determine the approximate hysteretic curves, following parameters are necessary.

- I. Initial peak load point ( $\delta_{m0}, H_{m0}$ )
- II. The parameter  $\beta_1$  and  $\beta_2$ , which determine the deterioration curve.
- III. The initial elastic stiffness  $K_{e0}$  and parameter  $\gamma$ , which can predict the descending of  $K_e$  by  $\sum \delta_d$ .
- IV. The parameter  $\mu$ , which predicts the shift of peak load point.

#### 3. Quasi-static tests

The parameters for hysteretic model can be obtained from the results of cyclic loading test or FEM cyclic loading analysis. The quasi-static tests for box section steel pier columns are conducted for this purpose.

##### 3.1. Test specimens and loading methods

###### 3.1.1. Test specimens

The test specimens are made by the steel grade of SM490. Six mm thick steel plates are used to make square section piers with 450mm width. There are 2 ribs behind each surfaces of the box section to stiffen the panel from local buckling. Three kinds of specimens, which have different diaphragm intervals as 450mm,

225mm and 150mm, are prepared. Names of these specimens describe using their diagram interval, as D450, D225 and D150. Two specimens for each type are used for the cyclic loading tests. Figure 6 and Figure 7 shows the side view and the section view of specimens. The sizes and parameters of specimens are listed in Table 1. The width-thickness ratio parameter  $R_R$ ,  $R_F$  and the length-to-slenderness ratio parameter  $\lambda$  are calculated by following equations.

$$R_R = \frac{b}{t} \sqrt{\frac{\sigma_y}{E} \frac{12(1-\nu^2)}{\pi^2 k_R}} \quad (14)$$

$$R_F = \frac{b}{t} \sqrt{\frac{\sigma_y}{E} \frac{12(1-\nu^2)}{\pi^2 k_F}} \quad (15)$$

$$\lambda = \frac{2h}{r} \sqrt{\frac{\sigma_y}{E}} \quad (16)$$

$$k_R = 4n \quad (17)$$

$$k_F = \frac{(1 + \alpha^2)^2 + n\gamma_l}{\alpha^2(1 + n\delta_l)} \quad (18)$$

where  $\alpha$  is the aspect ratio of the plate,  $\alpha_0$  is the limit aspect ratio,  $\gamma_l$  is supplement member's stiffness rate,  $\delta_l$  is the area rate of one supplement member divided by whole section area,  $b$  and  $t$  is the width and thickness of a panel,  $r$  is the equivalent radiation of the cross section,  $h$  is the effective height of the test model pier,  $k_R$ ,  $k_F$  are the buckling coefficient shown in Eq.(17) and (18) respectively.

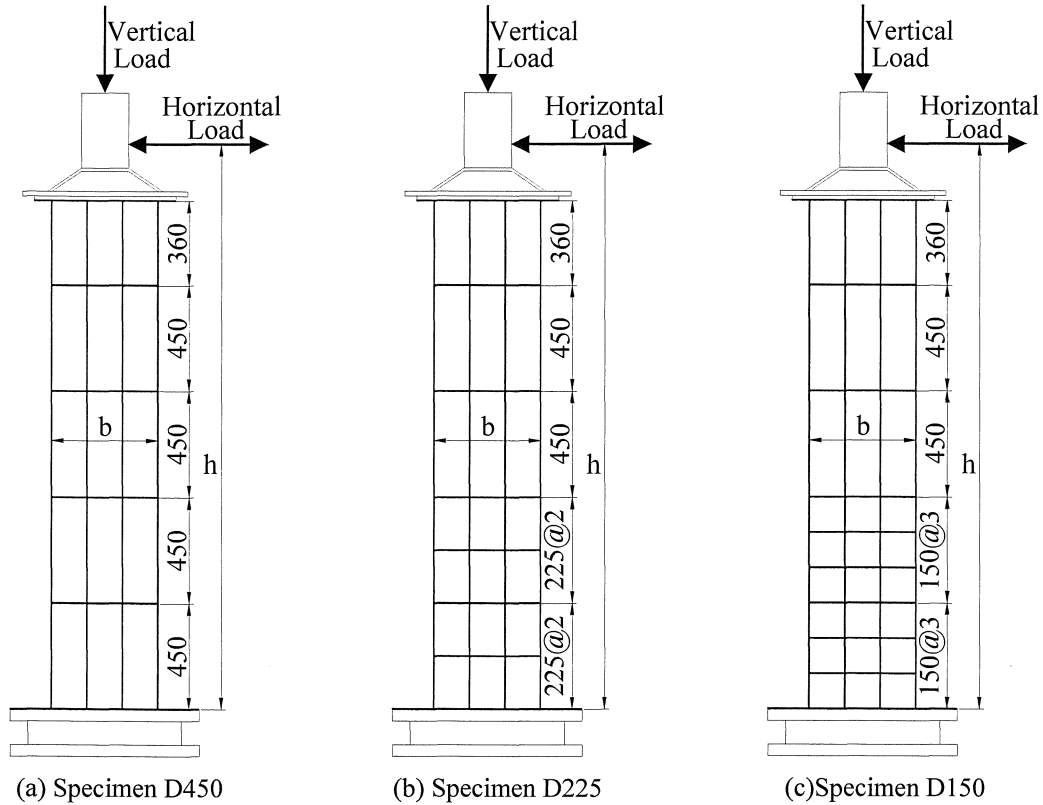


Figure 6. The side views of specimens

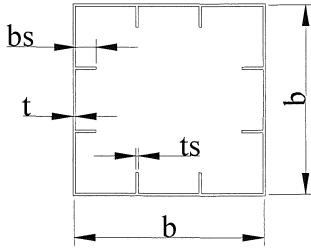


Fig.7 The section view for all types of specimens

Table 1. Geometry sizes of specimens

Specimen	D450	D225	D150
b (mm)	450		
t (mm)	6		
$b_s$ (mm)	55		
D (mm)	450	225	150
$t_s$ (mm)	6		
h (mm)	2400		
A (mm <sup>2</sup> )	13300		
I (mm <sup>4</sup> )	$4.06 \times 10^8$		

Table 2. Geometry parameters of specimens

Specimen	$R_R$	$R_F$	$\lambda$	$\lambda_s$	$\gamma/\gamma^*$
D450	0.517	0.336	0.397	0.368	2.5
D225		0.170		0.183	10.5
D150		0.113		0.123	26.7

### 3.1.2. Loading method

Each specimen is subjected to the prescribed horizontal displacement pattern under a constant axial vertical load  $P$  of 0.15 times the squash load  $P_y$ .  $P_y$  (=4320 kN) is obtained from the nominal yield stress of SM490.

Four strain gages are pasted at 30mm distance from the bottom to measure the strain at the base of specimen. The yield displacement and strength are recorded when the strain at the base of each specimen reaches the yield strain  $\epsilon_y$ .

As a basic loading pattern, the specimen is loaded by controlling displacements as  $\pm 0.5\delta_y, \pm 1\delta_y$  (3 cycles),  $\pm 1.5\delta_y, \pm 2\delta_y$  (3 cycles), and so on. After experienced the peak value of horizontal load ( $H_m$ ), the loading displacement is increased by  $1\delta_y$  in each cycle until collapse.

The test D450-1 is the first quasi-static test using specimen D450, which loading pattern is such that the

loading displacement is increased by  $1\delta_y$  after 2 loading cycles before peak load in this test.

### 3.2 Test Result

Tensile coupon test results for each specimen type are listed in Table-3.

Table 3. Result of material tests

Specimen	$\sigma_y$ (N/mm <sup>2</sup> )	$\epsilon_y$ ( $\times 10^{-6}$ )	E (N/mm <sup>2</sup> )	$\sigma_u$ (N/mm <sup>2</sup> )
D450	415	1961	$2.25 \times 10^5$	568
D225	409	2011	$1.98 \times 10^5$	546
D150	384	1858	$2.07 \times 10^5$	505

For each specimen type, two quasi-static tests are conducted, using the specimen named as D450-1, D450-2, D225-1, D225-2, D150-1 and D150-2. The yield displacement  $\delta_y$  and yield force  $H_y$ , which are defined by the yield strain, and the initial elastic stiffness  $K_{e0}$  obtained as average for various specimen types from these tests are listed in Table 4.

In Figure 8 (a)-(f), the solid lines illustrate the  $H$ - $\delta$  loading history, where  $H$  and  $\delta$  are normalized by  $H_y$  and  $\delta_y$  respectively. From these figures, the initial peak load points ( $\delta_{m0}, H_{m0}$ ) can be obtained and the average of two test results for same type of specimens are obtained and listed in Table 4.

Following the method presented above, the relationships between  $H_{eq}$  and  $\delta_d$  are obtained from the quasi-static tests as presented in Figure 9 (a)-(c). From these figures, approximate deterioration curves are found by applying Eq.(8). The parameters  $\beta_1$  and  $\beta_2$  in Eq.(8) are determined by the least-squares method and listed in Table 4.

It can be seen from these figures that the deterioration curves are fitted with Eq.(8) for all type of specimens with different parameters  $\beta_1, \beta_2$ .

By the same way, the deterioration relationships of  $K_e$ - $\delta_d$  and their regression by Eq.(10) are presented in Figure 10 (a)-(c).

The relationships of  $\delta_p^* - \delta_p$  of test data and the approximate relation applying Eq.(13) are presented in Figure 11 (a)-(c).

From these figures, it can be seen that the proposed approximate equations, Eq.(10) and (12), accurately present the deterioration for the elastic stiffness and the displacement shift in peak load points. For all specimens, the specific values of the parameter  $\gamma$ , which decide the deterioration of  $K_e$  with  $\delta_d$ , and the values of parameter  $\mu$  (which decide the displacement shift of peak load point  $\delta_p^*$  by deterioration displacement  $\delta_p$ ) are obtained and listed in Table 4.

Table 4. Hysteretic parameters from quasi-static tests

Specimen	$\delta_y$ (mm)	$H_y$ (kN)	$K_{e0}$ (kN/mm)	$\delta_{m0}$ (mm)	$H_{m0}$ (kN)	$\beta_1$ ( $\times 10^{-2}$ )	$\beta_2$ ( $\times 10^{-3}$ )	$\gamma$ ( $\times 10^{-2}$ )	$\mu$
D450	12.4	201	16.3	42.7	344	-6.47	1.51	-2.55	0.623
D225	15.0	238	15.9	38.5	408	-9.06	3.41	-0.186	0.871
D150	14.8	242	16.4	36.2	390	-8.3	2.79	-1.21	0.904

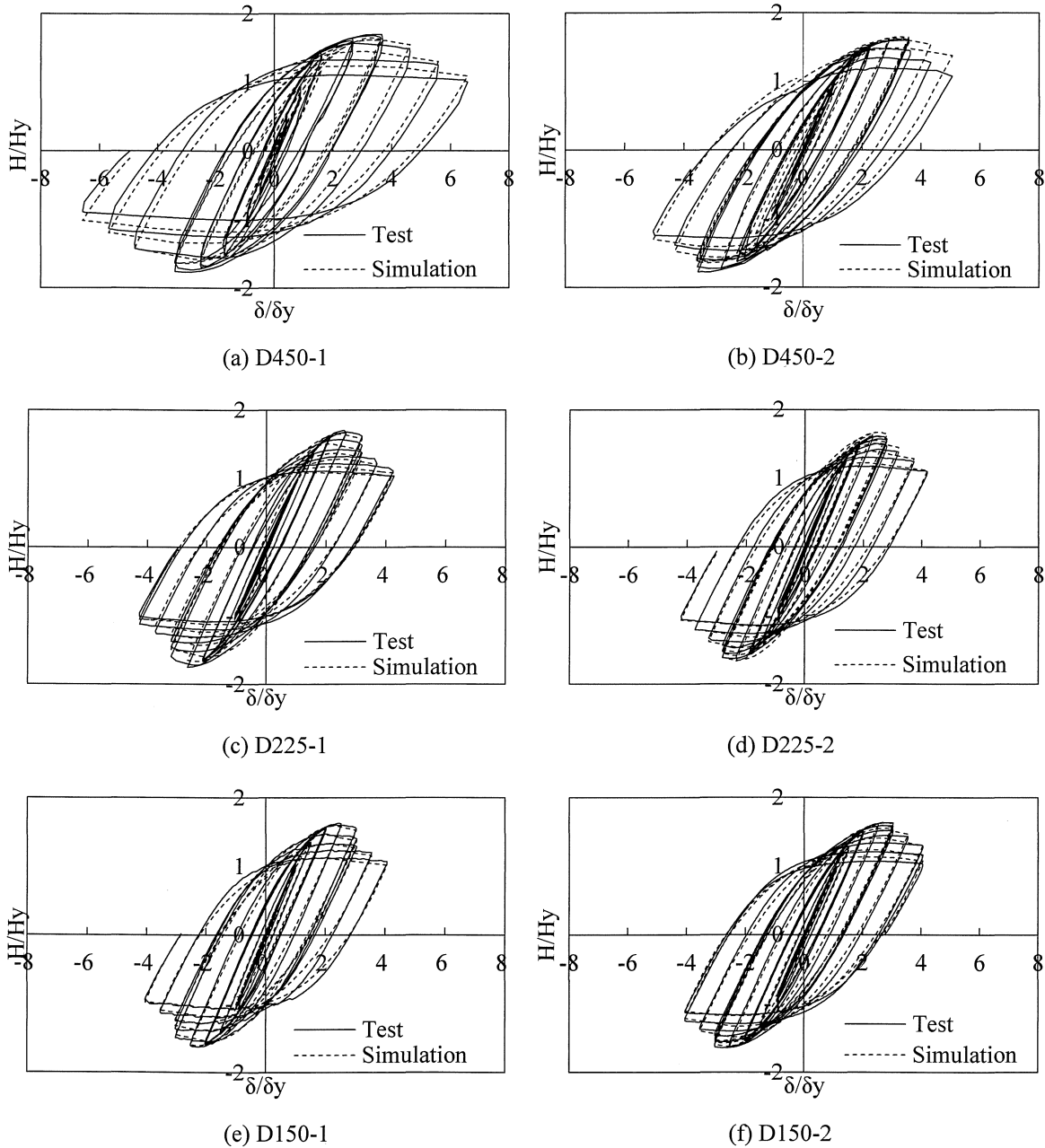


Figure 8.  $H-\delta$  loading history

After obtaining all necessary parameters, the  $H-\delta$  loading histories were simulated and compared with the displacements history of the quasi-static tests, as shown

in Fig.11 (a) ~ (f). It can be seen from these figures that the results of simulation based on curve approximate hysteretic model are very similar to the loading tests.

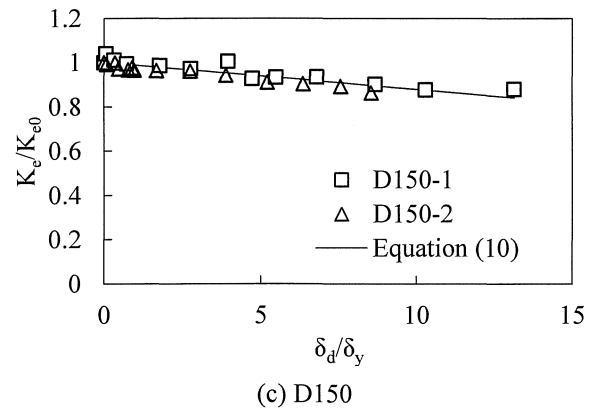
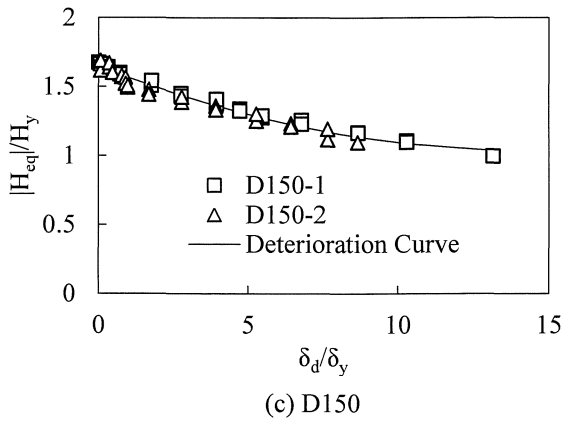
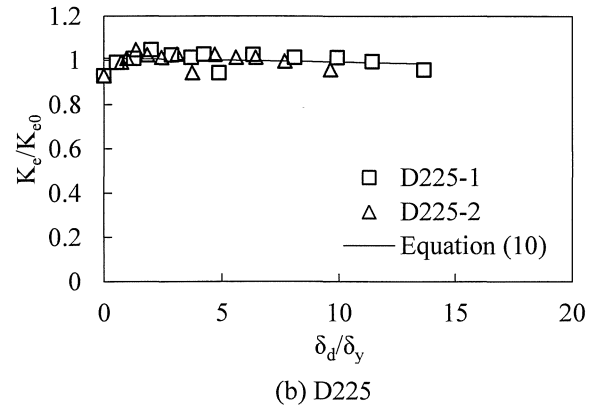
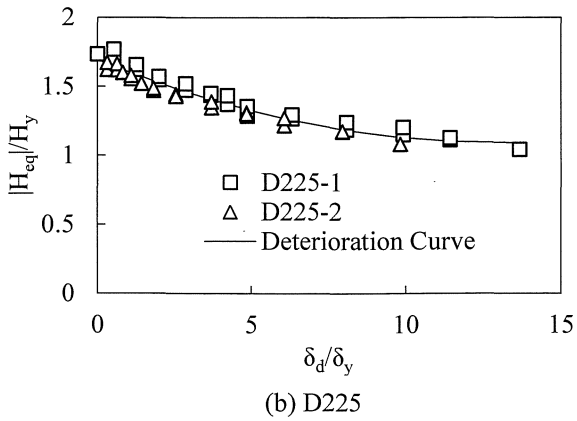
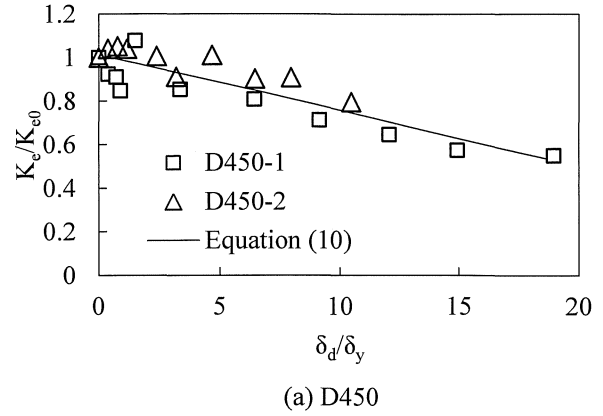
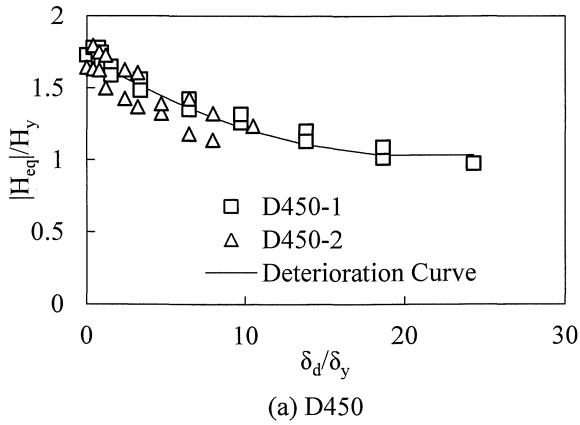


Figure 9. The relationships of  $H_{eq}$  and  $\delta_d$

Figure 10. Deterioration of elastic stiffness

#### 4. Hybrid Test

The hybrid loading tests are conducted to compare with simulation results by the curve approximate hysteretic model for steel piers. The specimens (D450, D225, D150) are used with the scale rate  $S=4$  for real bridge piers to obtain the corresponding restoring force of the full scaled single bridge pier model. The Newmark  $\beta$  method ( $\beta=1/6$ ) is applied to solve the vibration equation as a displacement prediction procedure using initial stiffness, under the time interval of  $\Delta t=0.01$  sec and the damping ratio of 0.05.

Hybrid tests and simulations are performed using six accelerograms of the Kobe Earthquake: NS and EW components recorded in Japan Meteorological Agency

(JMA-NS, JMA-EW, Ground Type I); NS and EW components recorded in Japan Railway Takatori station (JRT-NS, JRT-EW, Ground Type II); NS and EW components recorded in Port-island Kobe Bridge (PKB-NS, PKB-EW, Ground Type III). Program of the hybrid tests and simulations are listed in Table-5.

#### 5. Comparison of tests and simulations

The inelastic time history seismic response analysis with the proposed curve approximate hysteretic model is conducted to simulate hybrid tests. The hysteretic loops, response displacement time histories, maximum response displacements, residue displacements and energy absorptions are compared with the result of simulation to



evaluate the accuracy of the curve approximate hysteretic model.

Figure 12 shows the hysteretic loops and time histories of response displacement obtained by test and simulation as well. Solid lines in Figure 12 show the result of test, and dashed lines show the result from simulation.

The hysteretic loops based on hysteretic model are obtained to be very similar with the test results. The response displacement time histories obtained by simulation also precisely agree with tests, whereas in cases of No.1, No.2, No.6 and No.7, there are differences in response after the maximum displacement.

In these cases, bridge piers are excited by accelerograms of JRT (NS and EW), and caused the response over 10 cycles of severe plastic loops. The hysteretic loops are difficult to predict in severe plastic cycles. The accumulation of error is considered as the reason of the above difference in response.

The maximum response displacement ( $\delta_{max}$ ) may be one of the most important indicators in the response performance based seismic design for steel piers. The accuracy of analysis method mainly accounts for the precision of the prediction of maximum response displacement of piers. Figure 13 shows a comparison of the maximum response displacement between tests and simulation. As can be seen, the maximum response displacements due to the simulations are almost as same as that of hybrid tests.

The average error in maximum response displacement between simulations and hybrid tests is merely 5%, and the largest difference is less than  $1\delta_y$ .

The residual displacement ( $\delta_r$ ) is a main indicator in estimation of the recovery capacity of the bridge pier after strong ground motion. Figure 14 shows comparison of test and simulation in residual displacement, where the residual displacement of simulation predicted the tests results almost correct, with the absolute average discrepancy of only  $0.35\delta_y$ .

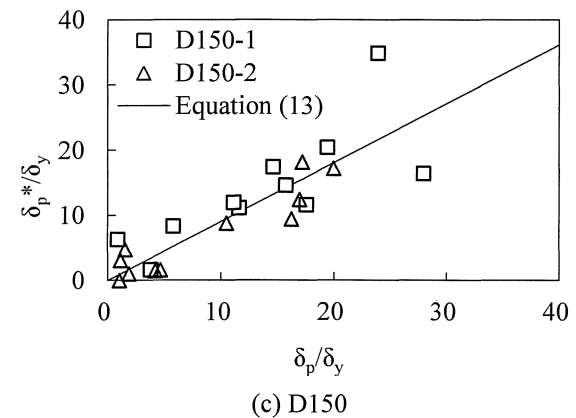
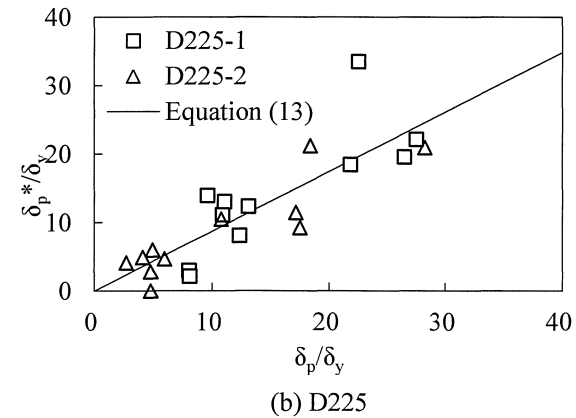
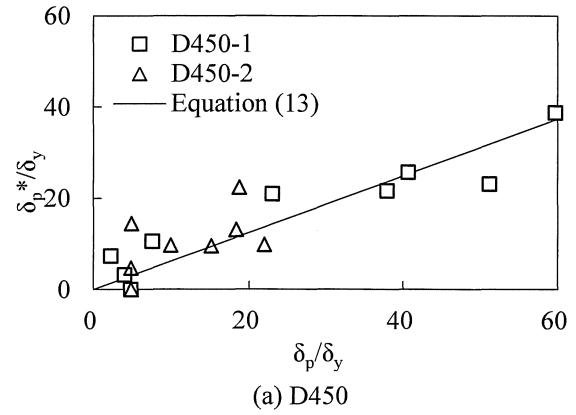
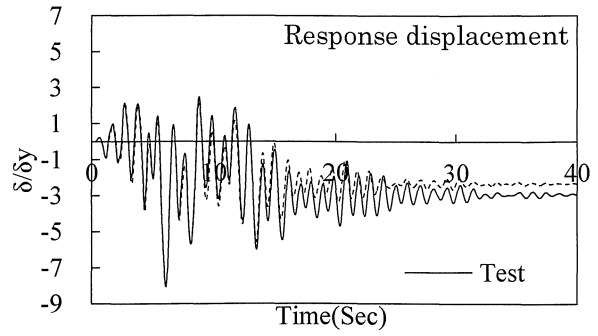
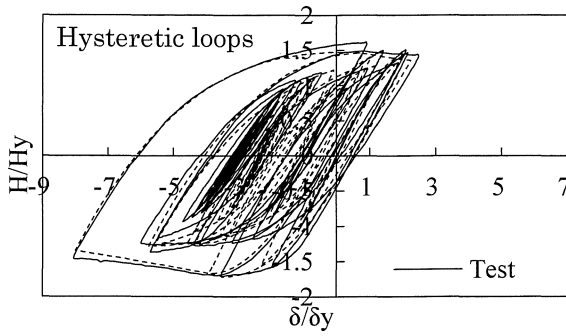


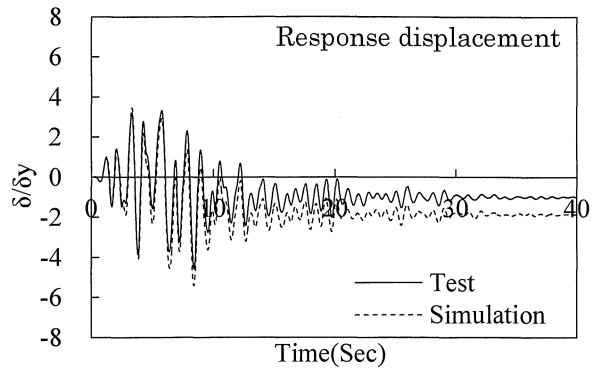
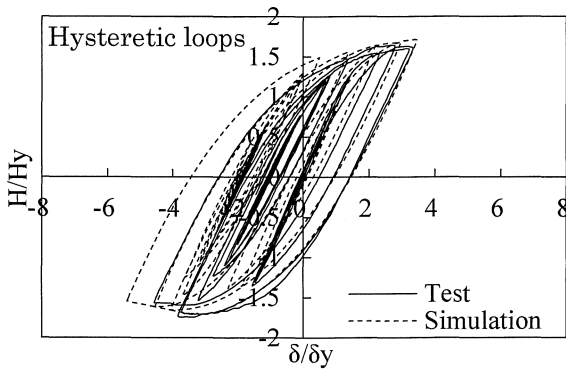
Figure 11. Shift of peak load point after deterioration

Table 5. Tests and Simulation Numbers and their Settings

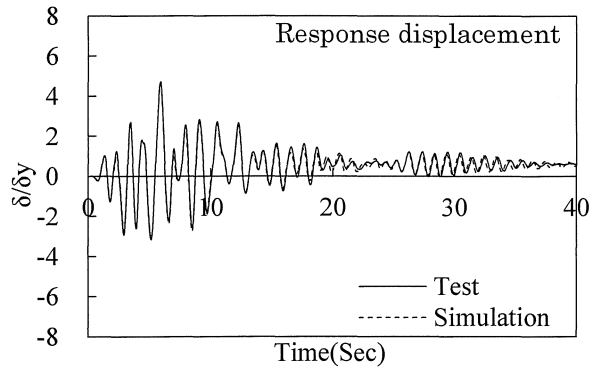
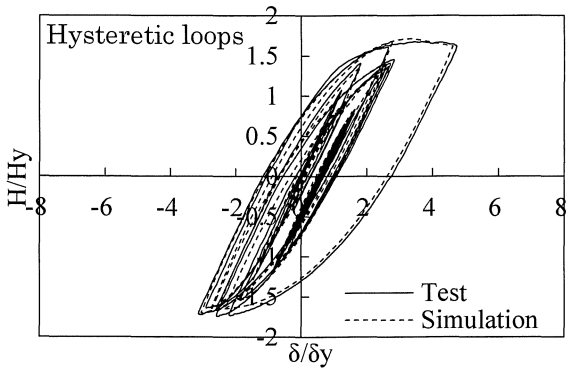
Specimen Type	S	Excitation Accelerograms					
		JMA (Ground Type I)		JRT (Ground Type II)		PKB (Ground Type III)	
		NS	EW	NS	EW	NS	EW
D450	4	--	--	No.1	No.2	--	--
D450	6	--	--	--	No.3	--	--
D225	4	No.4	No.5	No.6	No.7	No.8	No.9
D150	4	--	--	No.10	No.11	--	--



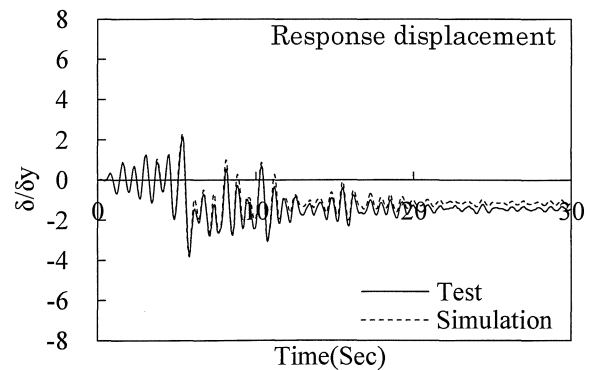
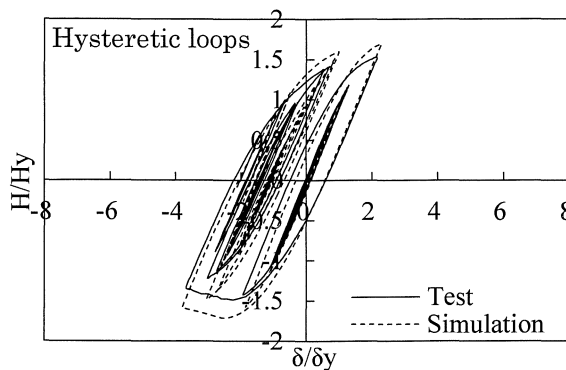
(a) No.1 (D450, S=4, JRT-NS)



(b) No.2 (D450, S=4, JRT-EW)

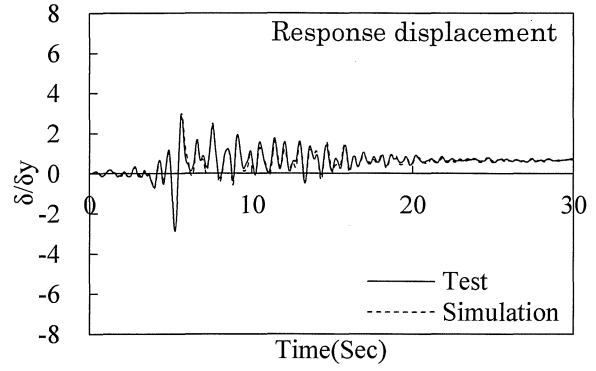
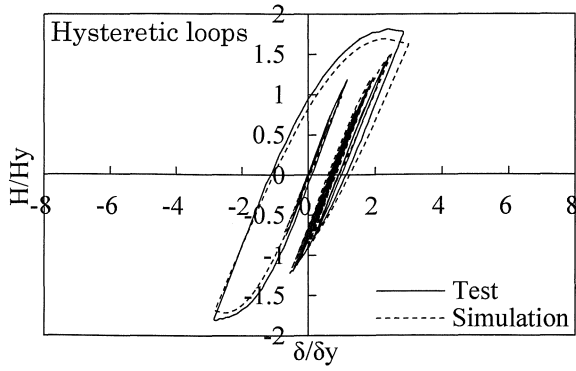


(c) No.3 (D450, S=6, JRT-EW)

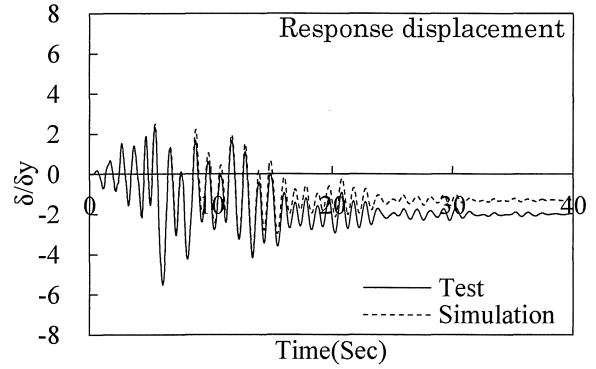
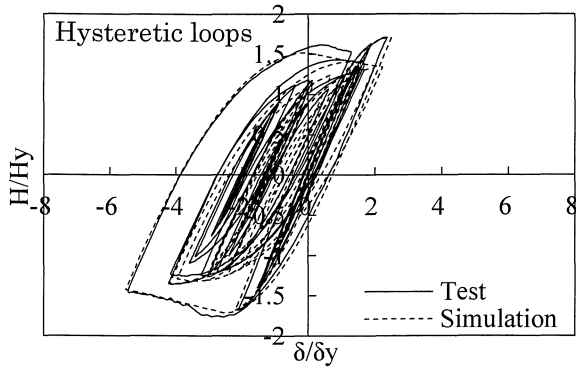


(d) No.4 (D225, S=4, JMA-NS)

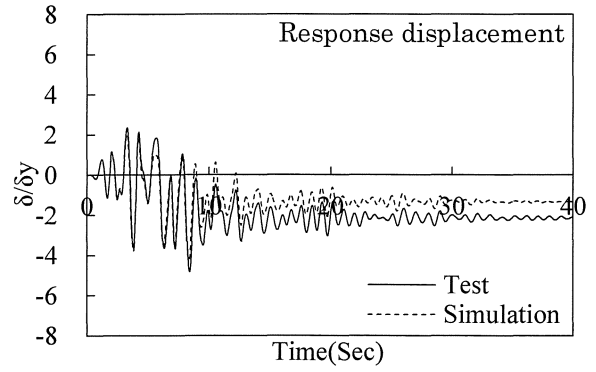
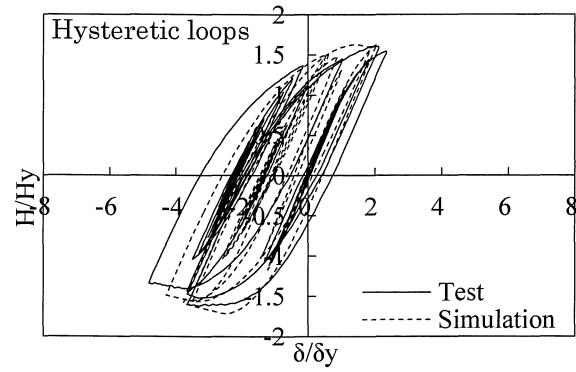
Figure 12. Hysteretic loops and response displacement time histories



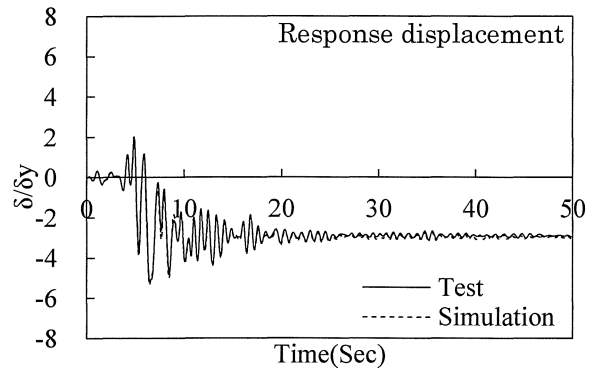
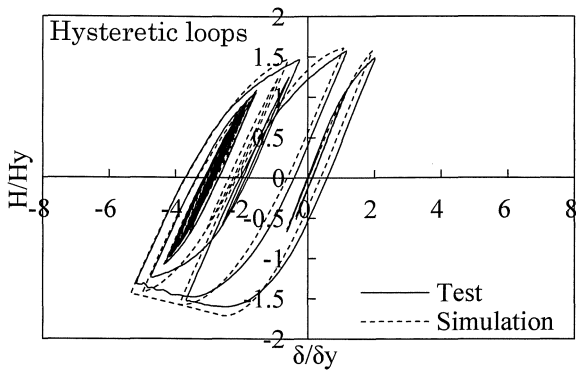
(e) No.5 (D225, S=4, JMA-EW)



(f) No.6 (D225, S=4, JRT-NS)

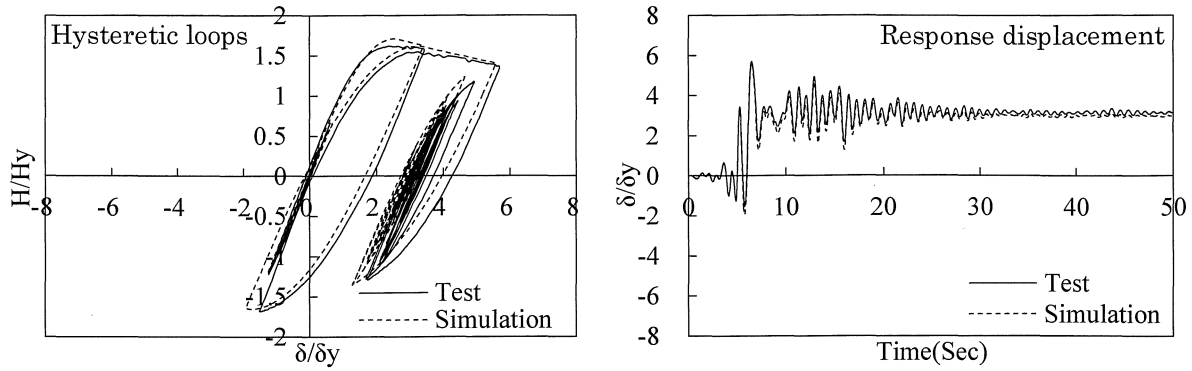


(g) No.7 (D225, S=4, JRT-EW)

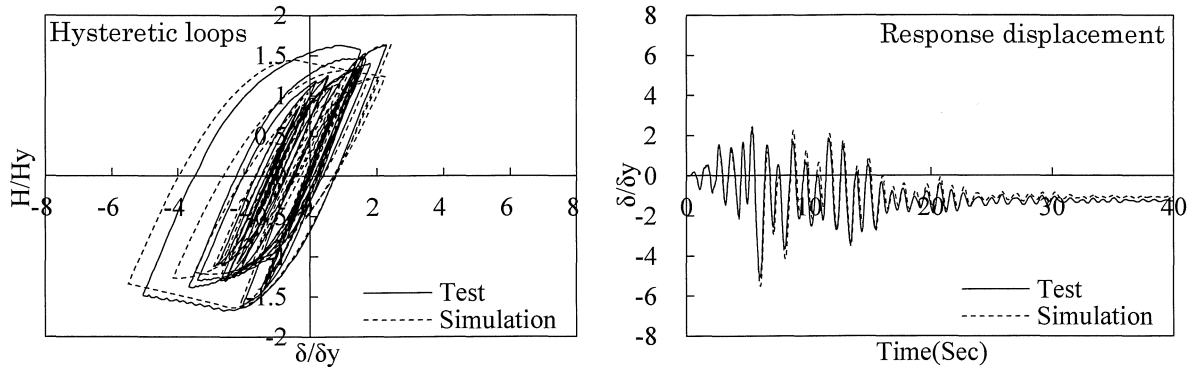


(h) No.8 (D225, S=4, PKB-NS)

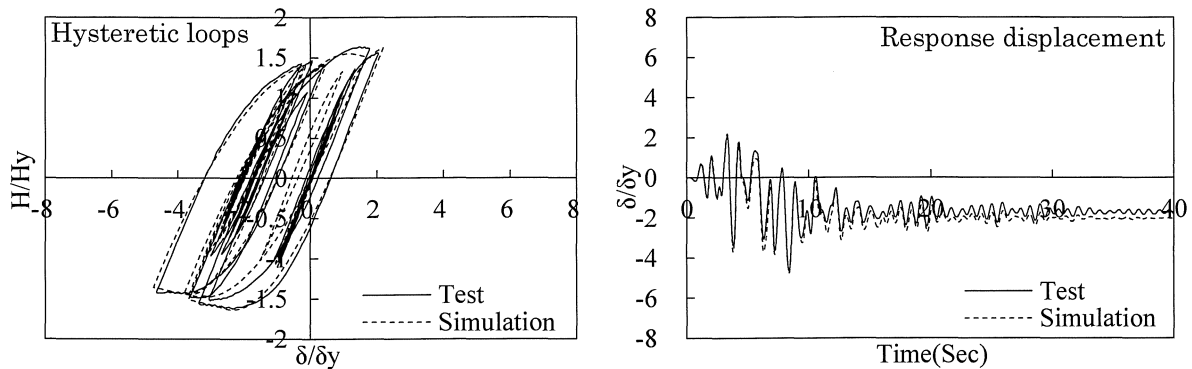
Figure 12. Hysteretic loops and response displacement time histories (Continue)



(i) No.9 (D225, S=4, PKB-EW)



(j) No.10 (D150, S=4, JRT-NS)



(k) No.11 (D150, S=4, JRT-EW)

Figure 12. Hysteretic loops and response displacement time histories (Continue)

Comparison in energy absorption of bridge pier under seismic excitation between tests and simulations is indicated in Figure 15. The energy absorption due to the curve approximate hysteretic model provides almost as same results as that of the hybrid test. The average error is merely 3%.

## 6. Conclusion

In this study, a curve approximate hysteresis model for steel bridge pier columns is proposed. The inelastic cyclic and deterioration behaviors of steel pier columns are investigated, taking into account of the P- $\delta$  effect. Based on a series of quasi-static and hybrid tests, the

accuracy of seismic response simulation applying the proposed curve approximate hysteretic model was discussed. It may be concluded from this study as follows.

- (1) The horizontal force-displacement relationship of steel pier columns is approximated by polynomial curves. It can estimate well the behavior of steel piers subjected to seismic excitations.
- (2) The first peak load point of steel pier can be considered as a constant point in the H- $\delta$  hysteresis relationship.

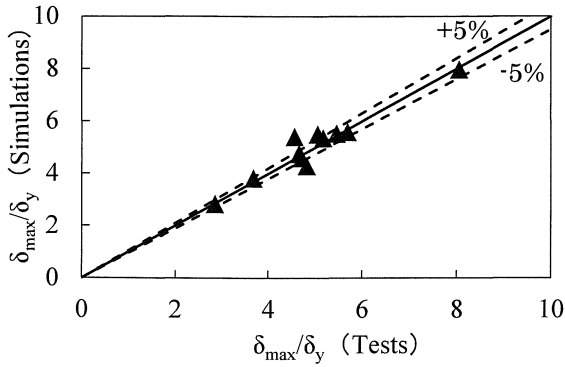


Figure 13. Comparison in maximum displacement

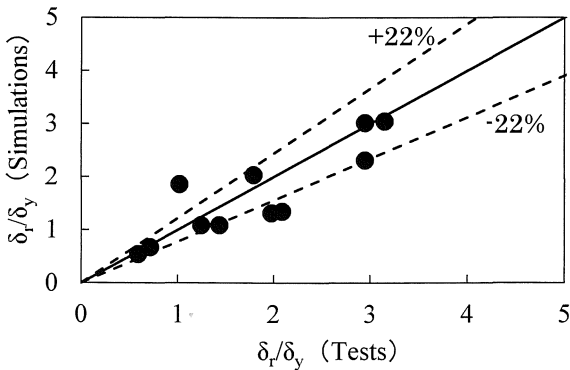


Figure 14. Comparison in residual displacement

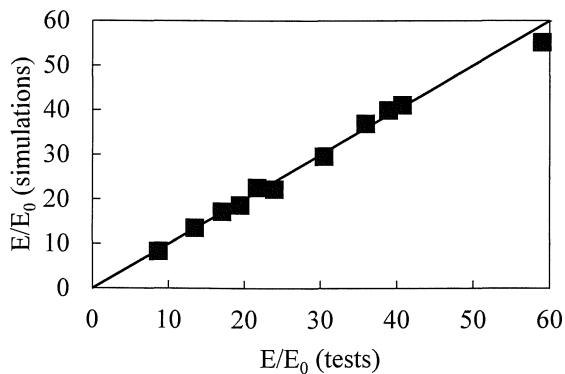


Figure 15. Comparison in energy absorption ( $E/E_0$ )

- (3) The average difference between the hybrid tests and the simulations for the maximum response displacement, the residual displacement and the energy absorption are 5%, 22% and 3% respectively.
- (4) The load-displacement hysteretic curve due to approximate hysteretic model can precisely evaluate the seismic response and the damage of steel pier columns under strong ground motions.

#### Reference:

Usami, T., Imai, Y., Aoki, T. and Itoh, Y. (1991). "An Experimental study on the Strength and Ductility of Steel Compression Member under Cyclic Loading" *Journal of Structure Engineer, JSCE*, 37(A), 93-106

Usami, T., Mizutani, S., Aoki, T., Itoh, Y. and Yasunami, H. (1992). "An Experimental study on the Elasto-Plastic Cyclic Behavior of Stiffened Box Members" *Journal of Structure Engineer, JSCE*, 38(A), 105-117

Usami, T., Banno, S., Zetsu, H. and Aoki, T. (1993). "An experimental study on the Elasto-Plastic Behavior of Compression Members under Cyclic Loading –Effect of Loading Program" *Journal of Structure Engineer, JSCE*, 39(A), 235-247

Suzuki, M., Usami, T. and Takemoto, K. (1995). "An Experimental study on Static and Quasi-Static Behavior of Steel Bridge Pier Models" *Structure Eng./Earthquake Eng., JSCE*, No.505(I-103), 99-108

Aoki, T., Ohnishi, A. and Suzuki, M. (2007). "Experimental study on the Seismic Resistance Performance of Rectangular Cross Section Steel Bridge Piers subject to Bi-Directional Horizontal Loads" *Journal of Structural Engineering, JSCE*, Vol.63(No.4), 716-726

Iemura, H. (1985). "Development and Future Prospect of Hybrid Experiments" *Structure Eng./Earthquake Eng., JSCE*, 356(I-3), 1-10

Saizuka, K., Itoh, Y., Kiso, E. and Usami, T. (1995). "A Consideration on Procedures of Hybrid Earthquake Responses Test taking account of the Scale Factor" *Structure Eng. / Earthquake Eng., JSCE*, No.505(I-30), 179-190

Usami, T., Saizuka, K., Kiso, E. and Itoh, Y. (1995). "Pseudo-Dynamic Tests of Steel Bridge Pier Model under Severe Earthquake" *Structure Eng./Earthquake Eng., JSCE*, No.519(I-32), 101-113

Suzuki, M., Usami, T., Terada, M., Itoh, T. and Saizuka, K. (1996). "Hysteresis Models for Steel Bridge Piers and their Application to Elasto-Plastic Seismic Response Analysis" *Structure Eng. / Earthquake Eng., JSCE*, No.549(I-37), 191-204

Kindaichi, T., Usami, T., Satish, K. (1998). "A hysteresis model based on Damage Index for steel bridge piers" *Journal of Structure Engineer, JSCE*, Vol.53(A), 667-678

Liu, Q.Y., Akira, K. and Usami, T. (1999) "Parameter Identification of Damage-based Hysteretic Model for Pipe-section Steel Bridge Piers" *Journal of Structural Engineering, JSCE*, 45(A), 1005-1016

Aoki, T., Suzuki, M. and Tanaka, T. (1998) "Multi-Curve Model for Steel Pier Hysteretic Curve" *Proceedings of the Second Symposium on Nonlinear Numerical Analysis and its Application to Seismic Design of Steel Structures, Vol.2*, 271-274

Usami, T. and Japan Society of Steel Construction (2006) "Seismic Resistance and Seismic control Design Guideline of Steel Bridge" *Gijyututou Press*, 128-129  
*Design Specifications of Highway Bridges (Part V. Seismic Design)*, Japan Road Association, March 2002

*Design Specifications of Highway Bridges (Part II. Steel Bridge)*, Japan Road Association, March 2002

Sibata, M. (2003) "Latest Seismic Resistance Analysis"

Morihaku Press

- Public Work Research Center of Japan, (2006) "The Manual of Bridge Seismic Resistance Dynamic Design-Dynamic Analysis, Basic and Application of Seismic Resistance Design"
- Satish, K., Usami,T.(1994) "A Note On The Evaluation Of Damage In Steel Structures Under Cyclic Loading" Journal of Structural Engineering , ASCE, 40(A), 178-188
- Ishizawa,T. and Iura,M. (2006). "One-Dimension Analysis of Box Section Steel Bridge Piers" Journal of Structural Engineering, JSCE, Vol.62(No.2), 288-299
- Fukaya,S., Ono,K., Shen,C., Murakosi,J. and Nishigawa,K.(2000). "Study on M- $\Phi$  Model for Steel Piers with Box Section Based on Cyclic Loading Experiments" Structure Eng./Earthquake Eng., JSCE, 37(A), 93-106
- Iura,M., Kumagai,Y. and Komaki,O.(1997). "Ultimate Strength of Stiffened Cylindrical Shells Subjected to Axial and Lateral Forces", Structure Eng./Earthquake Eng., JSCE, No.556, 107-118
- Dang J., Morita S., Aoki T., Suzuki M.: The Curve Hysteretic Model for the Quasi-Hybrid Test of Steel Piers, Summary Collection of the 64<sup>th</sup> Annual Academic Lecture Conference, JSCE,2009